

# Characterization of a *KCNB1* variant associated with autism, intellectual disability, and epilepsy

OPEN

Jeffrey D. Calhoun, PhD\*  
Carlos G. Vanoye, PhD\*  
Fernando Kok, MD  
Alfred L. George, Jr., MD  
Jennifer A. Kearney, PhD

Correspondence to Dr. Kearney:  
jennifer.kearney@northwestern.edu

## ABSTRACT

**Objective:** To perform functional characterization of a potentially pathogenic *KCNB1* variant identified by clinical exome sequencing of a proband with a neurodevelopmental disorder that included epilepsy and centrotemporal spikes on EEG.

**Methods:** Whole-exome sequencing identified the *KCNB1* variant c.595A>T (p.Ile199Phe). Biochemical and electrophysiologic experiments were performed to determine whether this variant affected protein expression, trafficking, and channel functional properties.

**Results:** Biochemical characterization of the variant suggested normal protein expression and trafficking. Functional characterization revealed biophysical channel defects in assembled homotetrameric and heterotetrameric channels.

**Conclusions:** The identification of the *KCNB1* variant c.595A>T (p.Ile199Phe) in a neurodevelopmental disorder that included epilepsy with centrotemporal spikes expands the phenotypic spectrum of epilepsies associated with *KCNB1* variants. The *KCNB1*-I199F variant exhibited partial loss of function relative to the wild-type channel. This defect is arguably less severe than previously reported *KCNB1* variants, suggesting the possibility that the degree of *KCNB1* protein dysfunction may influence disease severity. *Neurol Genet* 2017;3:e198; doi: 10.1212/NXG.000000000000198

## GLOSSARY

**MW** = molecular weight; **WT** = wild type.

De novo *KCNB1* variants have been identified in patients with early-infantile epileptic encephalopathy-26.<sup>1-6</sup> The *KCNB1* gene is intolerant of missense variation and is ranked among the top 1%–2% of intolerant genes in the genome ( $Z_{\text{mis}} = 5.15$ ).<sup>7</sup> *KCNB1* encodes  $K_{\text{V}}2.1$ , a voltage-gated potassium channel expressed in a wide variety of neuron types.  $K_{\text{V}}2.1$  channels underlie the principal delayed rectifier current in many neurons and contribute to regulation of neuronal excitability, especially during high-frequency firing.<sup>8</sup> Characterization of previously reported *KCNB1* patient variants revealed a variety of functional defects, including loss of ion selectivity, reduced conductance, and dominant negative effects.<sup>4-6</sup>

Here, we report a novel *KCNB1* variant in an individual with a neurodevelopmental disorder that included epilepsy and centrotemporal spikes on EEG. The proband exhibits infrequent seizures that are well controlled on sulthiame, intellectual disability, disruptive behavior, and autistic traits. Functional characterization revealed partial loss-of-function biophysical defects of assembled homotetrameric and heterotetrameric channels.

**METHODS** Standard protocol approvals, registrations, and patient consents. Anonymized genetic and clinical summaries were reported to us following clinical whole-exome sequencing. A review by the Northwestern University International Review Board

\*These authors contributed equally to this work.

From the Department of Pharmacology (J.D.C., C.G.V., A.L.G., J.A.K.), Northwestern University Feinberg School of Medicine, Chicago, IL; Human Genome and Stem Cell Research Center (F.K.), Biosciences Institute, University of Sao Paulo, Brazil; and Mendelics Análise Genômica (F.K.), Sao Paulo, Brazil.

Funding information and disclosures are provided at the end of the article. Go to [Neurology.org/ng](http://Neurology.org/ng) for full disclosure forms. The Article Processing Charge was funded by the NIH.

This is an open access article distributed under the terms of the Creative Commons Attribution-NonCommercial-NoDerivatives License 4.0 (CC BY-NC-ND), which permits downloading and sharing the work provided it is properly cited. The work cannot be changed in any way or used commercially without permission from the journal.

deemed this study as exempt, nonhuman subject research. Consent for release of deidentified medical information was obtained by physicians in accordance with local institutional policies.

**Plasmids and transfection.** I199F was introduced into a human  $K_v2.1$  cDNA clone pIRES2-DsRed-MST- $K_v2.1$ -WT.<sup>6</sup> Wild type (WT) and I199F were transiently expressed in CHO-K1 cells by electroporation (Maxcyte STX). Briefly, 7.5  $\mu$ g of cDNA was mixed with  $10 \times 10^6$  viable cells resuspended in 100  $\mu$ L of electroporation buffer, transferred to a processing assembly (OC-100R10), and electroporated using the CHO protocol. Coexpression was achieved by coelectroporation with 5  $\mu$ g each of pIRES2-DsRed-MST- $K_v2.1$ -I199F and pIRES2-eGFP- $K_v2.1$ -WT using the same protocol. Following electroporation, cells were incubated for 72 hours before experiments.

**Cell-surface biotinylation.** Surface proteins on CHO-K1 cells expressing WT or mutant  $K_v2.1$  were labeled with membrane-impermeable Sulfo-NHS-Biotin (Thermo Fisher Scientific, Waltham, MA), as described.<sup>6</sup> Total and surface fractions were analyzed by immunoblotting using mouse anti- $K_v2.1$  (1:250; K89/34; Neuromab, Davis, CA), mouse anti-transferrin receptor (TfR) (1:500; H68.4; Invitrogen, Carlsbad, CA), and rabbit anti-calnexin (1:250; H70; Santa Cruz, Dallas, TX) primary antibodies. AlexaFluor680 and 790-conjugated goat anti-rabbit and goat anti-mouse IgG secondary antibodies were used (1:20,000; Jackson ImmunoResearch, West Grove, PA). Blots were analyzed using the OdysseyCLx system and ImageStudio software (LICOR). Calnexin immunoreactivity was absent from the cell-surface fraction, confirming the selectivity of biotin labeling for cell-surface proteins. Normalized total, surface, and total:surface ratios were compared using one-way analysis of variance.

**Electrophysiology.** Automated planar-array patch-clamp recording was performed with the SyncroPatch 768 PE system (Nanion, München, Germany). Recording solutions are shown in table 1. Pulse generation was performed with PatchControl software (Nanion), and whole-cell currents were acquired at 5 kHz and filtered at 1 kHz. Currents were not leak subtracted. Fast and slow capacitances were compensated using internal algorithms within PatchControl software. Whole-cell currents were measured from a holding potential of  $-80$  mV and elicited with depolarizing steps (500 milliseconds) from  $-80$  to  $+60$  mV (10 mV steps) followed by a step to 0 mV (tail currents, 250 milliseconds). Background currents were removed by digital subtraction of whole-cell currents recorded from nontransfected cells.

**Table 1** Solutions for electrophysiologic recording

	External, mM	Internal, mM
NaCl	140	10
KCl	4	50
KF	—	60
MgCl <sub>2</sub>	1	1
CaCl <sub>2</sub>	2	—
Glucose	5	—
EGTA	—	20
HEPES	10	10
pH	7.4	7.2

**Table 2** Biophysical channel properties of KCNB1-WT and KCNB1-I199F homotetramers and heterotetramers

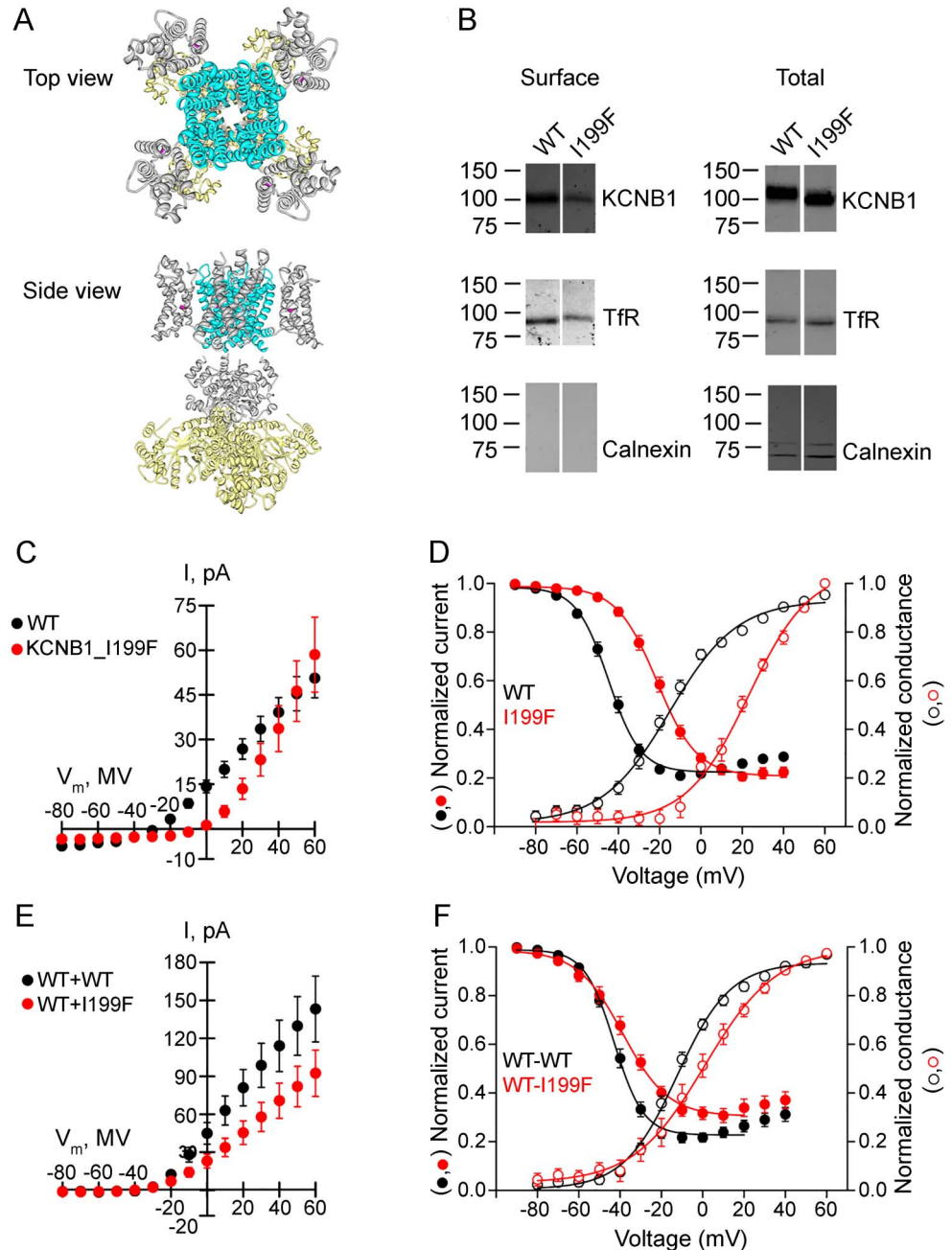
	$I_p^a$ pA/pF	Voltage dependence of activation		Voltage dependence of inactivation	
		$V_{1/2}$	k	$V_{1/2}$	k
<b>Homotetramer</b>					
KCNB1-WT	50.6 $\pm$ 6.6; N = 185	-12.9 $\pm$ 1.9; N = 63	16.7 $\pm$ 1.1; N = 63	-44.2 $\pm$ 1.4; N = 33	6.3 $\pm$ 0.2; N = 33
KCNB1-I199F	58.5 $\pm$ 12.6; N = 74; p = 0.548	+23.4 $\pm$ 1.7; N = 23; p < 0.001	14.0 $\pm$ 1.7; N = 23; p = 0.164	-21.4 $\pm$ 1.6; N = 26; p < 0.001	8.3 $\pm$ 0.3; N = 26; p < 0.001
<b>Heterotetramer</b>					
WT + WT	143.2 $\pm$ 26.0; N = 27	-10.9 $\pm$ 1.7; N = 26	12.9 $\pm$ 0.7; N = 26	-42.3 $\pm$ 1.4; N = 22	6.1 $\pm$ 0.3; N = 22
WT + I199F	92.4 $\pm$ 12.6; N = 40; p = 0.104	-1.9 $\pm$ 2.5; N = 31; p = 0.006	17.4 $\pm$ 1.4; N = 31; p = 0.009	-39.2 $\pm$ 2.3; N = 29; p = 0.146	7.5 $\pm$ 0.4; N = 29; p = 0.011

<sup>a</sup> Peak current.

To remove bias for expression efficiency or the functional level, homotetramer currents were analyzed from all cells with  $R_{\text{seal}} \geq 0.5 \text{ G}\Omega$ ,  $R_{\text{series}} \leq 20 \text{ M}\Omega$ , and  $C_m > 2 \text{ pF}$ . The peak current was normalized for cell capacitance and plotted against voltage to generate peak current density-voltage relationships. Voltage

dependence of activation and inactivation were evaluated only from cells with positive outward current values following background subtraction. Tail currents measured 5 milliseconds after stepping to 0 mV were normalized to the largest tail current amplitude and plotted against the depolarizing test potential

**Figure** Functional characterization of KCNB1-WT and KCNB1-I199F



(A) Location of the I199F variant mapped onto the crystal structure of a  $K_v2.1/K_v1.2$  chimera (PDB 29R9).<sup>10</sup> A channel tetramer is shown. I199F (magenta) lies in the S1 transmembrane segment of the voltage-sensing domain. (B) KCNB1-I199F is expressed and trafficked to the cell surface. Cell-surface expression was measured using cell-surface biotinylation of CHO-K1 cells transfected with wild-type (WT) or mutant  $K_v2.1$ . Total (5  $\mu\text{g}$  per lane) and surface fractions of  $K_v2.1$  were detected with the anti- $K_v2.1$  antibody. Endogenous TfR levels were measured as a loading control. Calnexin was present in total cell lysates, but not surface fraction, demonstrating selective biotinylation of extracellular proteins. The blot shown is representative of 3 independent experiments. (C) Current-voltage relationships measured for KCNB1-I199F ( $n = 74$ ) and WT homotetrameric channels ( $n = 185$ ). (D) Voltage dependence of activation and inactivation curves calculated for KCNB1-I199F ( $n = 23$ ) and WT ( $n = 63$ ) homotetrameric channels. (E) Current-voltage relationships measured for KCNB1-I199F ( $n = 40$ ) and WT ( $n = 27$ ) heterotetrameric channels. (F) Voltage dependence of activation and inactivation curves calculated for KCNB1-I199F ( $n = 31$ ) and WT ( $n = 26$ ) heterotetrameric channels.

(−80 to +60 mV). Normalized G-V curves were fit with the Boltzmann function:  $G = 1/(1 + \exp[(V - V_{1/2})/k])$  to determine the voltage for half-maximal activation ( $V_{1/2}$ ) and slope factor ( $k$ ). Voltage dependence of inactivation was assessed following a 5-second prepulse from −90 to +40 mV (10 mV steps) followed by a 250-millisecond step to +60 mV. Normalized peak currents measured at the +60 mV step were plotted against the prepulse voltage and fit with Boltzmann functions:  $I/I_{\max} = 1/(1 + \exp[(V - V_{1/2})/k])$  to determine the voltage for half-maximal inactivation ( $V_{1/2}$ ) and slope factor ( $k$ ). For heteromeric (WT + I199F) channels, peak current density-voltage relationships and voltage dependence of channel activation and inactivation were evaluated from cells with positive outward current values after background subtraction. Outliers ( $> \pm 2$  SDs) were not included. Results are expressed as mean  $\pm$  SEM.  $p$  Values for comparisons between the mutant and WT (Student  $t$  test) are listed in table 2 and in figure.

**RESULTS** Clinical whole-exome sequencing was performed in an adolescent with intellectual disability, disruptive behavior, autistic features, epilepsy and centrotemporal spikes on EEG. Seizures are infrequent and well controlled with sulthiame. Exome sequencing revealed a single de novo missense variant in *KCNB1* c.595A>T (p.Ile199Phe), which was confirmed by Sanger sequencing. This variant was absent in the ExAC and gnomAD databases containing exomes from 123,126 individuals unaffected by severe pediatric disease.<sup>7</sup> Isoleucine 199 is located in the S1 transmembrane segment of the voltage-sensing domain (figure, A) and is evolutionarily invariant through chordates.

Effects of the KCNB1-I199F variant on channel function were evaluated following transient expression. CHO-K1 cells expressing KCNB1-I199F had total and cell-surface expression similar to the WT, indicating that channels were expressed and trafficked to the cell surface (figure, B). KCNB1-I199F had a larger proportion of low-molecular-weight (MW) species relative to the WT in the total fraction (figure, B). Kv2.1 undergoes extensive multisite phosphorylation that affects apparent MW and function.<sup>8</sup> However, there was no apparent MW difference in surface fractions, suggesting that mutant and WT channels at the cell surface have similar posttranslational modifications.

Automated planar patch-clamp recording in parallel of I199F and WT homomeric channels resulted in characteristic voltage-dependent potassium currents with outward rectification and late inactivation. The current-voltage relationship was similar between I199F and WT (figure, C). I199F exhibited significant depolarizing shifts in the voltage dependence of activation and inactivation relative to the WT (figure, D). To mimic the heterozygous condition, we coexpressed KCNB1-I199F plus WT. Coexpression of KCNB1-I199F with the WT trended toward decreased current amplitudes between −10 mV and 60 mV (figure, E)

( $p = 0.104$ ). Furthermore, there was a significant depolarizing shift in voltage dependence of activation relative to the WT alone, without affecting voltage dependence of inactivation (figure, F). Details of the biophysical characterization are shown in table 2.

**DISCUSSION** The nature of channel dysfunction for KCNB1-I199F differs from previously reported *KCNB1* variants. I199F resulted in biophysical defects predicted to confer reduced channel availability due to shifts in the voltage dependence of activation, consistent with partial loss of function. By contrast, previously reported variants had complete loss of function, dominant negative effects, or loss of ion selectivity.<sup>4–6</sup> Previously characterized *KCNB1* variants were all located in the pore domain,<sup>4–6</sup> while I199F is the first reported variant located in the S1 transmembrane segment of the voltage-sensing domain. *KCNB1* variants have been reported in other voltage-sensing domain segments, but none have been functionally characterized to date.<sup>3</sup> However, variants in this domain of other voltage-gated potassium channels result in disease.<sup>9</sup> The I199F proband has neurodevelopmental and behavioral symptoms that are consistent with prior reports. However, seizures were reported to be infrequent and well controlled with sulthiame, whereas previously reported cases with pore variants had frequent, drug-resistant seizures.<sup>1,2,4–6</sup> This suggests the possibility that the variant type may influence the seizure phenotype and/or drug responsiveness. Consistent with this, a recent report suggests that the variant position (pore vs voltage sensor) influences the penetrance and severity of electroclinical and seizure phenotypes, while neurodevelopmental symptoms are present in all cases to date.<sup>3</sup> Larger cohorts with drug-response data will be necessary to investigate this link.

The phenotype spectrum associated with *KCNB1* variants will continue to expand as it becomes more widely screened. Correlating the clinical phenotype with channel dysfunction may provide insights into targeted therapeutic strategies.

#### AUTHOR CONTRIBUTIONS

Jeffrey D. Calhoun performed functional evaluation of the variant and wrote and edited the manuscript. Carlos G. Vanoye performed functional evaluation of the variant, performed statistical analysis of electrophysiology data, and edited the manuscript. Fernando Kok identified the *KCNB1* variant and edited the manuscript. Alfred L. George, Jr. conceived the study and edited the manuscript. Jennifer A. Kearney conceived the study, performed variant interpretation, and wrote and edited the manuscript.

#### ACKNOWLEDGMENT

The authors thank Katarina Fabre for technical support and the patient and family for their cooperation.

#### STUDY FUNDING

This work was supported by a grant from the NIH/National Institutes of Neurologic Disorders and Stroke to J.A.K. (R01 NS053792). The

funders had no role in study design, data collection and analysis, decision to publish, or preparation of the manuscript.

## DISCLOSURE

J.D. Calhoun receives fellowship support from the Dravet Syndrome Foundation. C.G. Vanoye consults for Nanion technologies. F. Kok has served on the editorial board of *Arquivos de Neuropsiquiatria*; holds a patent for Methylmalonic acid determination by tandem mass spectrometry using stable isotope; is an employee and shareholder of Mendelics Análise Genômica; and has been a speaker at NPC symposia from Actelion Pharmaceuticals. A.L. George, Jr. has served on a scientific advisory board of Amgen; has received travel funding from Praxis Precision Medicines, Inc.; has served on the editorial boards of *the Journal of Clinical Investigation*, *Heart Rhythm Journal*, and *the Journal of General Physiology*; is funded by the NIH, Merck Sharp & Dohme, St. Baldrick's Foundation, AHC Foundation, and Simon's Foundation; received research support from Xenon Pharmaceuticals and Dravet syndrome foundation; and consulted for Gilead Sciences and Xenon Pharmaceuticals. J.A. Kearney is funded by the NIH and Ovid Therapeutics; consults for Praxis Precision Medicine; received research support from Sage Therapeutics, Xenon Pharmaceuticals, and Parnomix, LLC; received license fee payments from Xenon Pharmaceuticals, Novartis, and Life Splice Technologies; and served on a scientific advisory board of Zogenix Inc. Go to [Neurology.org/ng](http://Neurology.org/ng) for full disclosure forms.

Received May 17, 2017. Accepted in final form October 15, 2017.

## REFERENCES

1. Allen NM, Conroy J, Shahwan A, et al. Unexplained early onset epileptic encephalopathy: exome screening and phenotype expansion. *Epilepsia* 2016;57:e12–e17.

2. de Kovel CG, Brilstra EH, van Kempen MJ, et al. Targeted sequencing of 351 candidate genes for epileptic encephalopathy in a large cohort of patients. *Mol Genet Genomic Med* 2016;4:568–580.
3. de Kovel CGF, Syrbe S, Brilstra EH, et al. Neurodevelopmental disorders caused by de novo variants in KCNB1 genotypes and phenotypes. *JAMA Neurol* 2017;74:1228–1236.
4. Saito H, Akita T, Tohyama J, et al. De novo KCNB1 mutations in infantile epilepsy inhibit repetitive neuronal firing. *Sci Rep* 2015;5:15199.
5. Thiffault I, Specca DJ, Austin DC, et al. A novel epileptic encephalopathy mutation in KCNB1 disrupts Kv2.1 ion selectivity, expression, and localization. *J Gen Physiol* 2015;146:399–410.
6. Torkamani A, Bersell K, Jorge BS, et al. De novo KCNB1 mutations in epileptic encephalopathy. *Ann Neurol* 2014;76:529–540.
7. Lek M, Karczewski KJ, Minikel EV, et al. Analysis of protein-coding genetic variation in 60,706 humans. *Nature* 2016;536:285–291.
8. Mohapatra DP, Park KS, Trimmer JS. Dynamic regulation of the voltage-gated Kv2.1 potassium channel by multisite phosphorylation. *Biochem Soc Trans* 2007;35:1064–1068.
9. Jen JC, Graves TD, Hess EJ, et al. Primary episodic ataxias: diagnosis, pathogenesis and treatment. *Brain* 2007;130:2484–2493.
10. Long SB, Tao X, Campbell EB, et al. Atomic structure of a voltage-dependent K<sup>+</sup> channel in a lipid membrane-like environment. *Nature* 2007;450:376–382.